© 2018. Published by The Company of Biologists Ltd | Journal of Experimental Biology (2018) 221, jeb168831. doi:10.1242/jeb.168831

RESEARCH ARTICLE

Foot-propelled swimming kinematics and turning strategies in common loons

Glenna T. Clifton* and Andrew A. Biewener

ABSTRACT

Loons (Gaviiformes) are arguably one of the most successful groups of swimming birds. As specialist foot-propelled swimmers, loons are capable of diving up to 70 m, remaining underwater for several minutes, and capturing fish. Despite the swimming prowess of loons, their undomesticated nature has prevented prior quantitative analysis. Our study used high-speed underwater cameras to film healthy common loons (*Gavia immer*) at the Tufts Wildlife Clinic in order to analyze their swimming and turning strategies. Loons swim by synchronously paddling their feet laterally at an average of 1.8 Hz. Combining flexion–extension of the ankle with rotation at the knee, loon swimming resembles grebe swimming and likely generates lift forces for propulsion. Loons modulate swimming speed by altering power stroke duration and use head bobbing to enhance underwater vision. We observed that loons execute tight but slow turns compared with other aquatic swimmers, potentially associated with hunting by flushing fish from refuges at short range. To execute turns, loons use several strategies. Loons increase the force produced on the outside of the turn by increasing the speed of the outboard foot, which also begins its power stroke before the inboard foot. During turns, loons bank their body away from the turn and alter the motion of the feet to maintain the turn. Our findings demonstrate that foot-propelled swimming has evolved convergently in loons and grebes, but divergently from cormorants. The swimming and turning strategies used by loons that allow them to capture fish could inspire robotic designs or novel paddling techniques.

KEY WORDS: *Gavia immer*, Paddling, Diving birds, Kinematics, Biomechanics, Maneuverability, Bird

INTRODUCTION

Loons excel at swimming, paddling their feet to dive underwater for more than 70 m (Schorger, 1947). They survive by capturing fish, a skill that requires a high level of maneuverability and speed. Yet, loons evolved from birds that use their hindlimbs for walking on land, repurposing their legs as paddles. Although producing propulsive forces underwater poses distinct physical challenges from walking, several independent lineages of birds have evolved foot-propelled diving, including grebes, cormorants, seaducks and extinct Hesperornithiformes (Zinoviev, 2011). Within extant foot-propelled diving birds, loons demonstrate a strong preference for large bodies of water and a particular intolerance for captivity. As a result, loon swimming has never been quantitatively studied. Yet, as one of nature's most agile foot-based swimmers, loons offer valuable insight into successful strategies for swimming and maneuvering underwater by means of foot-propelled paddling.

Diving birds face specific physical challenges to power underwater locomotion, leading to varying levels of specialization within foot-propelled diving birds. The most recent common ancestor of all extant birds was able to walk and fly, passing on to its descendants anatomical features to support the body against gravity while on land and reduce body mass for flight (such as hollow bones; Johnsgard, 1987). Yet, many of these characters limit swimming performance. All swimming birds must overcome buoyancy to dive, with adaptations to increase body density such as wettable feathers (Grémillet et al., 2005) or solid bones (Chinsamy et al., 1998). Birds that swim using their feet encounter particular physical challenges associated with the hindlimbs. The propulsive force generated by a foot depends on its speed, shape and surface area (Vogel, 2008). To maximize force, many foot-propelled birds have webbed or lobed toes, but large feet may make walking on land cumbersome. Because of these conflicting functional pressures on the hindlimb, foot-based diving birds face a trade-off with walking. As a result, foot-propelled swimming has independently evolved to differing levels of specialization, from many cormorants and seaducks that regularly spend time on land (Abourachid, 2001; White et al., 2008) to grebes and loons that can barely stand on solid ground (Johnsgard, 1987).

The loon family includes five extant, Holarctic species, including the common loon (*Gavia immer*), which breeds on lakes in northern North America and winters along the North American coasts (Johnsgard, 1987). Loons spend almost their entire life on the water, only venturing onto land to build and tend a nest near the shoreline. The common loon has been caught in fishing nets dozens of meters below the surface (Schorger, 1947), with diving durations recorded of over 2 min (Nocera and Burgess, 2002). However, loons prefer large territories (Barr, 1996), and adults do not survive well in captivity (Miller and Fowler, 2014). The technical challenges of studying loon swimming have impeded any prior analysis of how loons produce the forces necessary to swim using their feet.

Foot-based swimming has historically been considered to rely on drag force production (Blake, 1981), though recent studies of other specialized diving birds suggest an ability to generate lift forces. Steady fluid forces can be categorized into drag and lift. Drag forces resist motion through a fluid, acting opposite to the direction of movement and parallel to incident water flow. In contrast, lift forces act perpendicular to the incident water flow over a propulsive appendage. Previously, swimming using the feet was considered drag-based, with the foot paddling backwards to power forward motion (Baudinette and Gill, 1985; Blake, 1981; Fish, 1996; Vogel, 2008). Yet, recent studies of cormorant and grebe swimming show that the feet of specialized diving birds do not move backwards relative to still water, and therefore likely power swimming more

Concord Field Station, Department of Organismic and Evolutionary Biology, Harvard University, Bedford, MA 01730, USA.

*Author for correspondence (gclifton@fas.harvard.edu)

G.T.C., 0000-0002-5806-7254; A.A.B., 0000-0003-3303-8737

Received 22 August 2017; Accepted 9 August 2018

through lift- than drag-based forces (Johansson and Norberg, 2000, 2001, 2003; Ribak et al., 2004). However, grebes and cormorants likely use different mechanisms for producing lift because of divergence in the shape of the feet and orientation of the limb while paddling. With feet that resemble those of cormorants but exhibiting a similar level of aquatic specialization to grebes, how do loons swim compared with cormorants and grebes? Do loons also exhibit signs of producing lift forces for underwater propulsion?

To successfully capture prey, specialized foot-propelled diving birds must not only power straight swimming but also be highly maneuverable. All previous studies of foot-propelled diving birds restricted subjects to a straight tunnel, though one study included a single vertical obstacle (Johansson and Norberg, 2001; Ribak et al., 2004, 2008). While informative, such experiments do not measure natural maneuverability in foot-propelled birds. Other freely swimming aquatic animals, from fish to penguins, demonstrate dramatic variation both in the sharpness and speed of turns and in the movement strategies to control turning (Fish, 2002; Fish et al., 2003; Hui, 1985). Animals that swim like loons with a rigid body and powering swimming with the feet, including rays and turtles, demonstrate a consistent pivoting strategy. These swimmers generate drag on the turning direction side of the body by extending the feet on the inside of the turn (often called the 'inboard feet') while continuing to generate thrust using the outside, 'outboard', feet (Fish and Nicastro, 2003; Rivera et al., 2006). However, unlike previously studied underwater foot-propelled swimmers, loons rely solely on two, not four, limbs for propulsion. Additionally, the unusual leg anatomy of loons restricts the feet to the very caudal edge of the body (Clifton et al., 2018), which positions the feet at a long distance from the center of mass enabling efficient maneuvering (Webb, 1988). It is therefore likely that loons use novel kinematic strategies to control maneuvers.

This study quantitatively evaluated swimming and turning strategies in loons for the first time. Using high-speed cameras in custom-built underwater camera cases, we filmed four healthy common loons freely swimming in a pool at the Tufts University Wildlife Clinic (North Grafton, MA, USA). Kinematic analysis of the body and hindlimbs during straight swimming revealed that loons power foot movement by ankle flexion and knee rotation. The feet are placed in a lateral position and appear to generate lift forces, similar to grebes. We also found that loons use head-bobbing to alternate stabilizing the head with augmenting the acceleration of the eye, likely enhancing visual localization of prey. To induce turns, loons use a combination of several strategies by modulating: (1) the speed of the outboard foot, (2) the relative timing of foot motion and (3) particular features of each foot's motion. Our findings provide the first evaluation of swimming in loons and reveal new mechanisms for controlling maneuvers using foot-based underwater swimming.

MATERIALS AND METHODS

Swimming recordings

The unpredictability of where loons swim combined with variable water clarity hinders the filming of loons underwater in the wild. However, adult common loons cannot be housed in captivity for long stays as they contract an often-fatal respiratory fungal disease when under acute stress (Miller and Fowler, 2014). Common loons, *G. immer* (Brunnich 1764), are listed as a species of concern in MA, USA (321 CMR 10:00, 2010), and threatened in NH, USA (Wildlife Action Plan, 2015), preventing the explicit capture of loons for observation in potentially life-threatening conditions. For these reasons, we filmed swimming loons at the Tufts University Wildlife Clinic during rehabilitation stays.

Between 2014 and 2016, four healthy loons were filmed at the Wildlife Clinic. Many of the loons brought into rehabilitation centers are not healthy enough for filming, quickly succumbing to lead poisoning from fishing tackle or traumatic injuries (Sidor et al., 2003). However, some loons are admitted with minimal injuries and are quickly released back into the wild. The Tufts Wildlife Clinic primarily receives loons during late autumn migration. The four loons filmed in this study sustained no major injuries and were filmed on the day of release, usually during the hours just prior to release. At the time of recording, the loons weighed between 2.5 and 3.2 kg, within the normal range for adults (Johnsgard, 1987). Therefore, the data presented here accurately represent swimming by healthy loons prior to being released from the rehabilitation clinic.

Loon swimming was filmed using two high-speed cameras (NR5S1, Integrated Design Tools, Tallahassee, FL, USA) in an indoor, 3.05 m diameter pool. The cameras were placed in custom-made underwater cases using adapted scuba dive boxes and 80/20 aluminium framing (Fig. S1). A wide-angle lens was attached to each camera (14 mm, f/3.2, Rokinon) and focused at a distance of 1.8 m in air. The effective lens focal length increases when submerged, resulting in an approximate in-focus depth of field of 1.3–2.7 m from the camera.

Specific measures were taken to minimize loon stress and loon–human interaction throughout the recording sessions in accordance with animal care protocols (Tufts IACUC G2013-103). Veterinary staff at the Wildlife Clinic removed the loon from the pool and placed it in a net-bottom cage while the camera stands and cameras were placed into the pool. The shared field-of-view of the cameras was calibrated using a custom-built submersible LED wand (30 cm length) filmed at 2 frames s^{-1} during at least 100 frames. As the loon was returned to the pool, length measurements of the beak, tarsometatarsus and digits were recorded. Body mass was measured during a check-in evaluation within 24 h before the recording. Once returned to the pool, each loon was filmed for up to 5 h, with regular breaks to turn off the extra, overhead halogen lights. An opaque sheet covering the netting above the pool (Fig. S1) prevented the loon from observing the researchers. Diving was often voluntary, though occasionally elicited by the researchers making a noise or moving the sheet. For each loon, 3–5 bait fish were released into the pool to elicit hunting dives. Recordings were collected using Motion Studio Software at 200 frames s^{-1} with a resolution of 2336×1728 pixels. The cameras were post-triggered and recorded a maximum of 572 frames, equivalent to 2.86 s. Loons were then often removed from the pool and directly prepared for transportation to be released. The field of view was calibrated again before the set-up was dismantled. Across four individuals, we recorded 159 swimming trials.

3D motion tracking

Calibration of the cameras for each day of filming was performed to convert 2D data from each camera to 3D information relative to a local coordinate system. Camera calibration was performed in MATLAB (The MathWorks, Natick, MA, USA) using easyWand5 (Theriault et al., 2014). Each wand calibration included at least 500, and up to 1200, digitized frames and was calculated by estimating the focal length and principal points of the cameras. The calibrations were aligned to vertical using a large, metal calibration object placed into the pool during calibration trials.

Of 159 recorded trials, 19 provided accurate 3D analysis of stride timing, body trajectory and hindlimb kinematics. These trials

included a diversity of swimming behaviors (straight swimming versus turning, descending in the water versus swimming along the floor) while ensuring that the bird was in focus and that an identifiable point on the body was visible in both views (more details provided below).

Each swimming stride consists of two phases: the power stroke and recovery phase. During the power stroke, the foot pushes backwards relative to the body to propel the bird forward. During the recovery stroke, the toes collapse onto each other and the foot is retracted cranially in an arc. The timing of 112 power strokes was determined by visually identifying toe abduction and adduction for each foot. Although some past studies on straight swimming define the power stroke based on the acceleration of the body (Johansson and Norberg, 2001), this measure does not account for variation between the feet, an important factor for turning. The start of the power stroke was identified as the point when the digits begin to abduct and the metatarsophalangeal (MTP) joint begins to extend. The end of the power stroke was defined as the point when the toes have mostly collapsed upon each other with the MTP joint moving cranially. A full stride was defined by the start of sequential power strokes by the same foot. Each stride was observationally classified as straight swimming or turning to the left or the right.

The body and head of the loon were tracked during portions of all 19 analyzed trials. Body tracking was possible for >30% of the duration of 36 swimming strides and for >70% of the duration of 23 strides. Six of the 19 trials included 3D limb tracking, providing a complete analysis of nine strides by the four birds. These nine strides included three during straight swimming (centripetal acceleration a_c<0.75 m s^{-1}, see below). The six turning strides (a_c>0.75 m s^{-1}) tracked four inboard feet and two outboard feet, capturing simultaneous strokes of both feet once. Body motion was completely tracked during all nine strides that yielded 3D limb analysis. In all, over 24,000 points were hand digitized for this study.

The body and limbs of each loon were manually tracked. Like many waterbirds, loons intensively preen and are highly sensitive to any disruption to the waterproofing of their feathers. In order to minimize stress to the birds, we could not attach markers onto the body to facilitate tracking anatomical planes of the loon. Instead, body motion was tracked most often using a feather coloration pattern at the midline of the caudal abdomen near the vent. When the vent was not visible in both cameras, either a point along the midline of the tail or a feather pattern along the back was used. The accuracy of tracking this point was always within less than a pixel. The head was tracked using either the eye or the tip of the beak. In loons, the upper hindlimb is incorporated within the abdominal body skin, making the hip and knee joints invisible (Clifton et al., 2018). However, these joints remain relatively immobile in flexion/extension as a result of skeletal structures stabilizing both joints (Hertel and Campbell, 2007; Wilcox, 1952), with most of the foot's motion stemming from flexion and extension of the ankle. The following hindlimb landmarks were tracked for at least one limb during each of the six trials: intertarsal 'ankle' joint, MTP joint and distal phalanx of digits II–IV.

Kinematics analysis

Power stroke time, stride time and duty factor were determined for each foot separately throughout the trial. Power stroke time was calculated by converting the number of frames between the beginning and end of the power stroke to duration (1 frame=5 ms). Stride duration was determined using the start of sequential power strokes as the beginning of toe abduction could be identified more accurately than toe collapse. A swimming duty factor was defined as the fraction of the stride used to power swimming, calculated as the power stride time divided by the stride time. For each of these variables, individual values were categorized as relating to straight swimming, the inboard foot during a turn or the outboard foot during a turn.

The tracked 3D motions of the body, head and hindlimb were smoothed and rotated relative to the forward motion and mediolateral axis of the loon. Custom-written MATLAB scripts applied a cubic spline ('smoothing spline' fit function, smoothing parameter=0.01) to the data. The relatively extreme smoothing parameter derives from a high frame rate relative to motion speed. Rotation matrices were defined and applied at each time step based on trajectory-based and anatomical axes. The x-axis was defined as the travel direction of the body. The y-axis corresponds to the line connecting the left and right ankle joints, representing the mediolateral plane of the bird assuming symmetrical or limited motion of the ankles relative to the body. The z-axis was calculated as the cross-product of the x- and y-axes, approximating the dorsoventral plane of the body. Loons swim with a downward anterior tilt of the body relative to the travel direction, resulting in a slight offset between the z-axis and dorsoventral plane of the loon. However, the consistency of the anterior tilt among trials supported the usefulness of x-, y- and z-axis comparisons across strides and individuals.

Average speed and turning characteristics were quantified for each stride. Previously, strides were defined for each foot using the start of the power stroke. Because the feet are paddled approximately synchronously but not exactly, full-body strides were defined using the earlier power stroke of the two feet. An average speed throughout each full-body stride was calculated only if the body had been tracked for over 70% of the stride (23 strides by four birds). The horizontal motion of the body was analyzed to quantify the extent of turning throughout each stride while neglecting the impact of buoyant forces. For strides in which at least 30% of the stride was digitized (36 strides by four birds), a 2D circle was best fitted to the horizontal trajectory (Taubin, 1991; Fig. S2). The radius of this circle was considered the average radius of curvature, r. While past studies have used a measure of instantaneous radius of curvature, we found this measure to overestimate the turning ability of the loon because of small deviations in the loon body trajectory. Using the average radius of curvature, stride angular velocity, ω, was calculated as:

$$\omega = \frac{u}{r}, \tag{1}$$

where u is the average horizontal speed throughout the stride and r is the average radius of curvature from the best-fit circle. From this, the centripetal acceleration acting on the loon throughout the stride, a_c, is:

$$a_c = \frac{u^2}{r}, \tag{2}$$

with units of m s^{-2} or expressed as multiples of gravitational acceleration, $\boldsymbol{g}$ (9.8 m s^{-2}). Together, these parameters give an approximate measure of the extent of turning throughout a stride. Strides with a_c>0.75 m s^{-2} were considered turns.

We statistically analyzed whether stride duration, power stroke duration and duty factor differ if loons swim straight or turn. We tested the influence of 'foot type' (straight, inboard foot, outboard foot) by fitting a linear mixed-effect model (fit type=REML) to the data and using a likelihood ratio test (MATLAB 2015b). The first

Journal of Experimental Biology (2018) 221, jeb168831. doi:10.1242/jeb.168831

model tested the influence of foot type while accounting for random effects from individual identification [Output~Foot+(1|Individual)]. These models were repeated, binning together inboard and outboard foot data, to compare straight swimming strides with all turning strides. The likelihood ratio tests were conducted using a model with the 'foot' as a fixed effect. We were unable to perform these analyses on foot splay (maximum distance between digits II and IV) because of a small sample size of tracked foot strides and relatively large anatomical variation among individual loons. To account for the influence of swimming speed on stride duration, power stroke duration and duty factor, we repeated the linear mixed-effect modeling using an extra fixed effect [Output~Foot+Speed+(1|Individual)]. Again, these models were performed with two separate stride groupings: straight versus inboard versus outboard and straight versus all turning. The likelihood ratio tests were conducted by removing the 'foot' and 'speed' effects independently. We determined significance using a cut-off of P=0.05. All values are listed as means±s.e.m.

RESULTS

Despite swimming in a confined pool, loons exhibited a range of normal and extreme behaviors. All four filmed loons frequently dived underwater voluntarily. When a fish was released into the pool, the loon would often capture the fish within 1–2 s before the fish could swim down from the surface. When multiple fish were released at the same time, the loon quickly captured each individual. Most of the loons demonstrated an acute fear of humans, and would dive instantly upon hearing or seeing the researchers; however, one of the loons showed no fear of humans, following the researchers around the pool and actively investigating the camera cases and stands. Each loon was filmed performing escape dives as well as voluntary relaxed dives.

Within the 19 tracked trials, loons swam at body speeds ranging from 0.16 to 0.86 m s^{-1}, averaging 0.56 m s^{-1}. Our video recording frame rate (200 Hz) provided a greater temporal resolution than previous studies on foot-propelled diving birds (50 Hz), enabling detailed analysis of the paddling timing and coordination. Stride duration ranged from 0.29 to 1.11 s, with an average of 0.55±0.02 s (Fig. 1B). Power stroke duration exhibited less variation, from 0.10 to 0.425 s, averaging 0.265±0.005 s (Fig. 1A). Duty factor varied from 0.16 to 0.86, with an average of 0.51±0.01 (Fig. 1C). In strides where the body was digitally tracked for more than 70% of the duration (36 strides by 4 birds), speed ranged from 0.29 to 0.89 m s^{-1}, and averaged 0.54±0.03 m s^{-1} (Fig. 1D).

Swimming hindlimb kinematics

The distal hindlimb was digitally tracked for eight complete strides in six trials, including two strides with tracking of both feet, resulting in a total of nine tracked strides. Despite some variation in the kinematics among individuals and trials, all strides demonstrate qualitatively similar limb motion during the power and recovery strokes (Figs 2 and 3; Movie 1). The foot (from the MTP to the tip of the digits) begins the power stroke lateral and somewhat ventral to the abdomen. Relative to the body, the foot then arcs caudally, dorsally and medially, ending the power stroke behind the body with the feet facing medially. This foot motion results primarily from extension of the tarsometatarsus at the intertarsal ankle, with only a small dorsal and lateral arc of the ankle relative to the body (Fig. 3, green). Note that, as depicted in Fig. 3, because of concurrent forward movement of the body, the foot experiences an overall forward motion (in the travel direction) relative to still water throughout the power stroke. The foot moves opposite to the travel direction only modestly, with comparatively large excursions in the ventral-to-dorsal and lateral-to-medial directions.

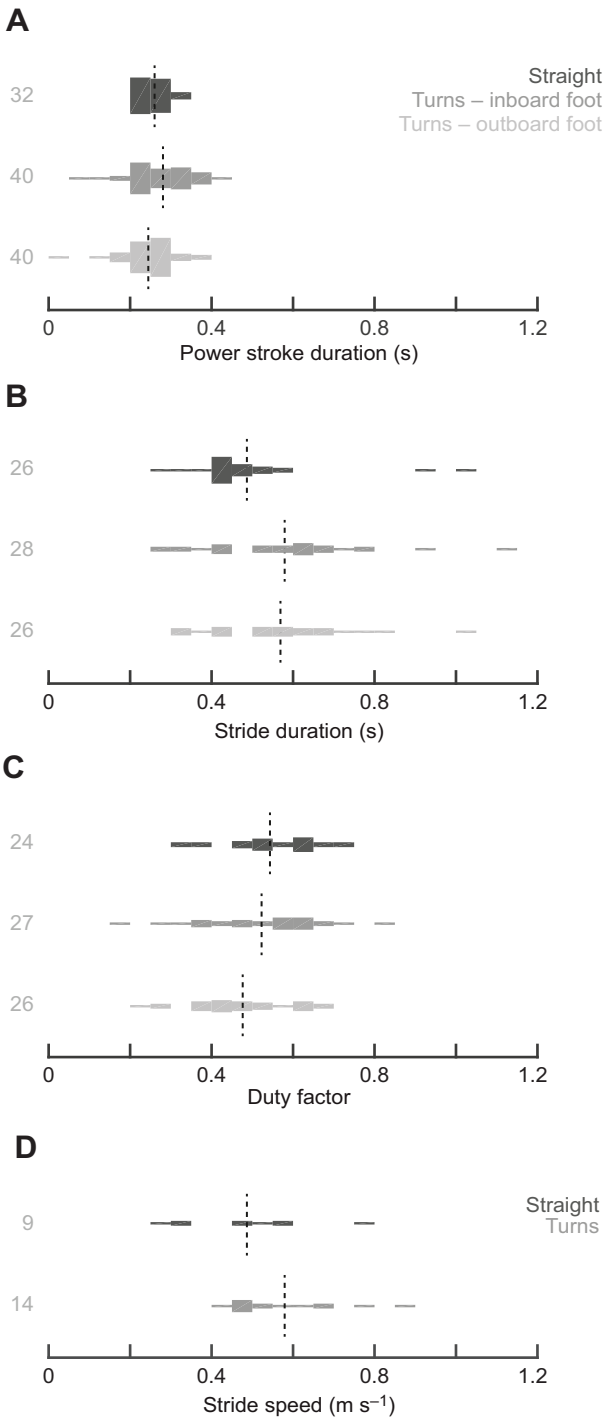

Fig. 1. Descriptive stride parameters of straight and turning swimming. Data from 112 strides in 19 trials across four loons showing values for straight swimming strides (dark gray), inboard foot of turning strides (medium gray) and outboard foot of turning strides (light gray). Violin plots (vertically mirrored histograms) show (A) power stroke duration, (B) stride duration, (C) duty factor and (D) body speed during strides. Data for stride speed are combined for inboard and outboard feet as turn data (medium gray). The width of each bin represents the number of data points, with values consistent across all panels. Dashed lines show the mean of each distribution. Numbers on the left list the total number of strides depicted in each plot.

Journal of Experimental Biology (2018) 221, jeb168831. doi:10.1242/jeb.168831

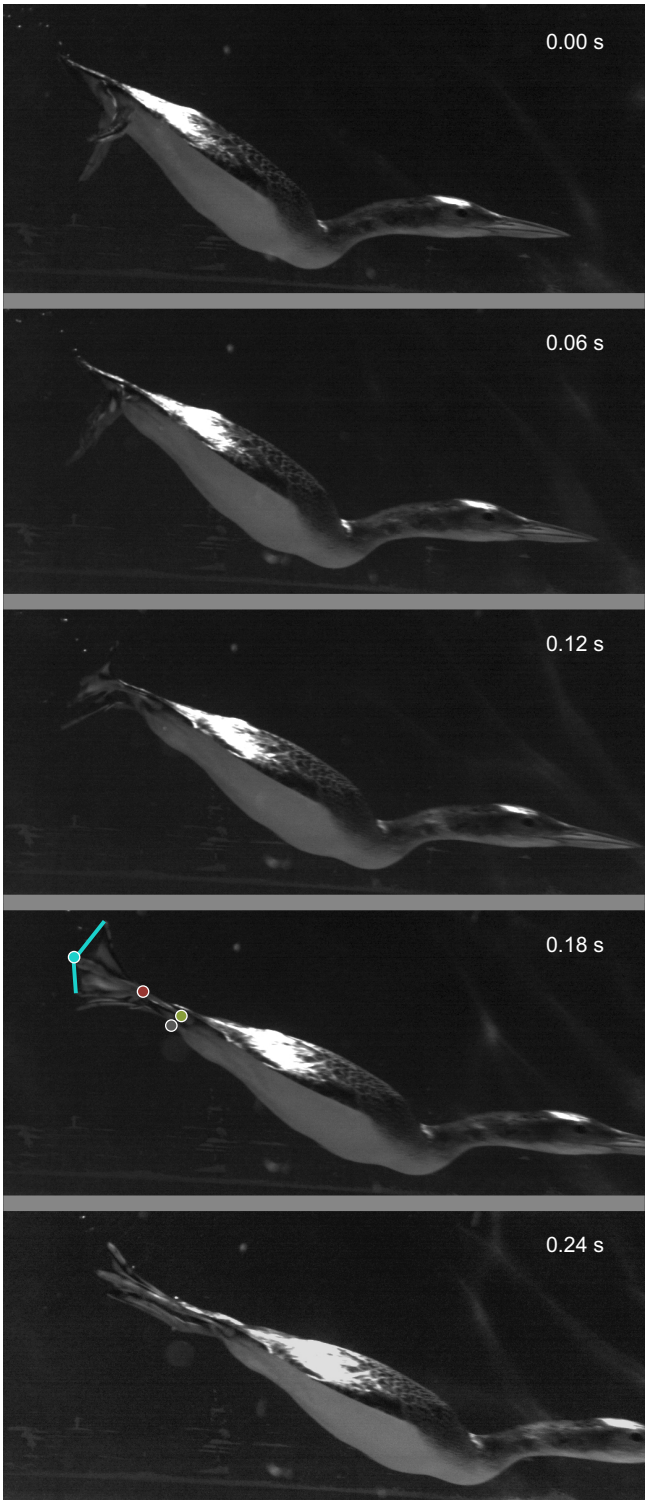

Fig. 2. Lateral view of loon power stroke during straight swimming. Each image is cropped from one camera's full field of view. The cropped area does not change among panels, representing loon motion relative to still water. Loons propel the body forward by extending the intertarsal ankle joints. Each foot travels in a lateral, backwards arc relative to the body as a result of extension at the intertarsal ankle joint. Throughout the power stroke, the digits abduct and extend at the metatarsophalangeal (MTP) joints. The power stroke ends as the ankle begins to flex, bringing the MTP joint forward and collapsing the digits onto each other. For this stride, the power stroke lasted 0.24 s. The circles and lines in the 4th panel denoting anatomical landmarks correspond to the colors used in Figs 3 and 7.

Throughout the power stroke, the digits extend and abduct at their MTP joint (Fig. 3, thin turquoise lines). In most trials, the digits hyperextend, reaching angles greater than 180 deg relative to the tarsometatarsus. However, in situations where the inboard foot is used as a rudder or executes a small power stroke compared with the outboard foot, the digits only somewhat abduct and never hyperextend. As the foot reaches a position behind the loon's body, the MTP flexes and the toes adduct, eventually collapsing onto each other and signaling the end of the power stroke.

During the recovery stroke, the MTP travels in an arc cranial, medial and slightly lateral relative to the body. The folded digits swing behind the tarsometatarsus. The ankle moves only slightly relative to the body during the recovery stroke. At the transition from the recovery to the power stroke, the forward-moving MTP slows down and reverses its motion to begin moving backwards relative to the body. At this point, the foot rotates from facing caudally during the recovery stroke to facing dorsally and medially during the power stroke.

Head bobbing

In approximately one-third of the 19 tracked trials, loons exhibited head bobbing. As their body glides forward during the recovery stroke, loons retract their neck to slow the velocity of the head relative to still water, sometimes achieving a stationary head position (Fig. 4; Movie 2). During the power stroke, the loons extend their neck, resulting in a faster acceleration of the head compared with that of the body. Within the 11 tracked head-bobbing strides, the head reached a maximum speed of 1.13 m s^{-1} and acceleration of 7.96 m s^{-2}, three times faster than those of the body (Fig. 4). Loons did not head bob during quick escape dives or sharp turns, but only during relatively horizontal swimming and while hunting bait fish.

Turning strategies

As filming occurred in a relatively small circular tank, most of the tracked trials recorded loons turning. Across all 36 strides with the body tracked for at least 30% of the stride, the average stride radius of curvature, r, was 0.42±0.07 m with an extreme value of 0.06 m, or approximately 0.07 body lengths (conservatively calculated based on a maximum body length of 0.91 m; Table S1). The average stride angular velocity (ω) was 92.4±10.9 deg s^{-1}, with an extreme of 287 deg s^{-1}. The average stride centripetal acceleration (a_c) was 0.80±0.55 m s^{-2}, with an extreme of 1.96 m s^{-2} or 0.20 $\boldsymbol{g}$.

Loons use several strategies to execute turns, including changing their body and wing positions, moving their feet at different timings, and varying factors that influence the force produced by each foot. In every observed turn, the body of the loon rolled out of the turn, resulting in the ventral belly facing into the turn (Fig. 5, Movie 3). For many turns, loons slightly extended their wings, particularly the outer wing during tight turns (Fig. 5). During one almost 180 deg turn, the loon also depressed its tail throughout the maneuver (Fig. 5C).

While turning, loons paddle the inboard and outboard feet at different times. In contrast, when swimming straight, loons synchronously paddle their feet, starting and stopping each foot's power stroke at approximately the same time (Fig. 6). However, during turns, loons almost always paddled the outboard foot 0.05–0.10 s before the inboard foot (Fig. 6), representing a temporal difference of 20–40% of power stroke duration. In some cases, loons extended the toes of the inboard foot when it was held lateral to the body, allowing the inboard foot to act as a rudder. In two trials, the use of the inboard foot as a rudder was extended over repeated paddling cycles of the outboard foot (Fig. 6, bottom row).

Journal of Experimental Biology (2018) 221, jeb168831. doi:10.1242/jeb.168831

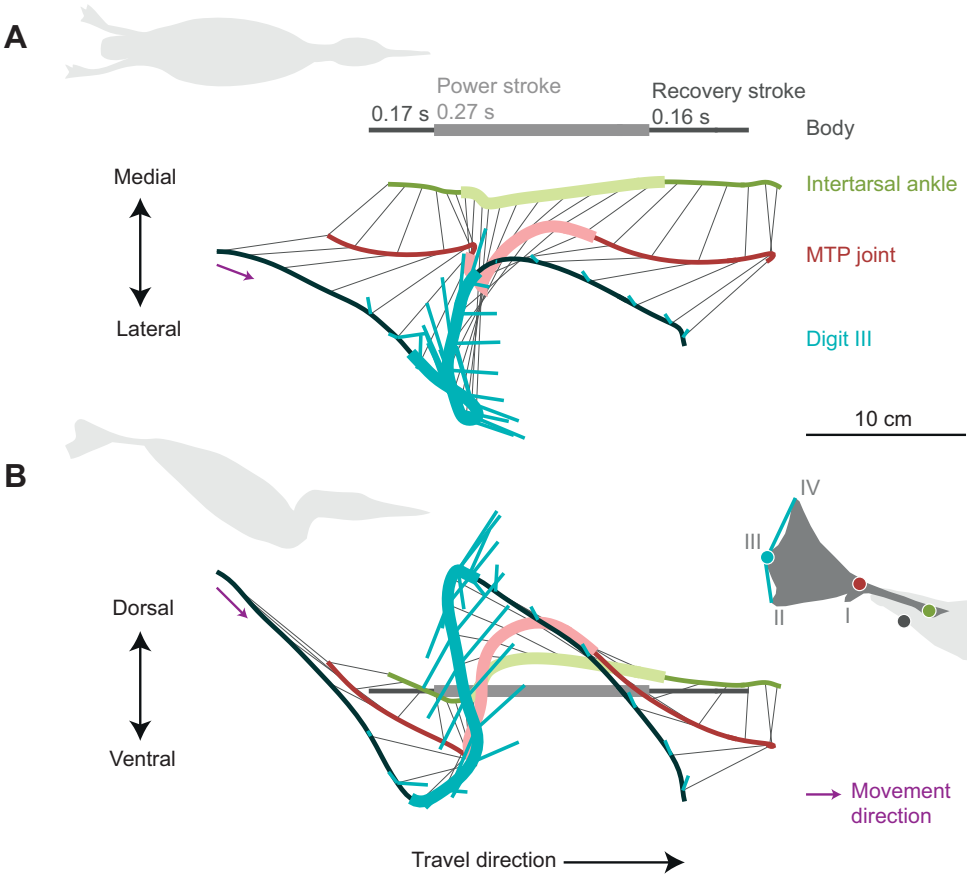

Fig. 3. Right foot motion during straight swimming relative to still water, rotated in reference to the loon. The traces show tracked motion relative to still water from a recovery stroke (thin lines), a power stroke (thick lines), then another recovery stroke of a loon swimming in a straight trajectory. The 3D data were rotated to be in reference to the travel direction (*x*-axis) and mediolateral plane (A, *y*-axis), with the 3rd coordinate axis representing a tilted dorsoventral plane (B, *y*-axis). (A) View of the right limb from above the loon showing the body (dark gray), intertarsal ankle (green), MTP joint (red) and tip of digit III (turquoise). (B) View of the right limb from the right side of the loon. The thin gray lines represent the two skeletal elements. Proximally, the tarsometatarsus connects the ankle to the MTP joint. Distally, digit III connects the MTP joint to the tip of digit III. Thin turquoise lines connect the tip of digit III to the tips of digits II and IV. Lines represent every 3rd frame (0.015 s). The 10 cm scale bar applies to both panels.

Although loons alter the relative timing of the feet when turning, only a few stride parameters varied between straight and turning strides. Without accounting for an influence of speed, no stride parameters showed kinematic variation. However, when accounting for both average swim speed and random effects from individual variation, a few variables demonstrated significant variation (Tables S2 and S3). The inboard foot used a longer power stroke compared with straight swimming strides (P=0.007; Table S3, Fig. S3). Power stroke duration significantly decreased with increasing stride speed for every model (Table S3).

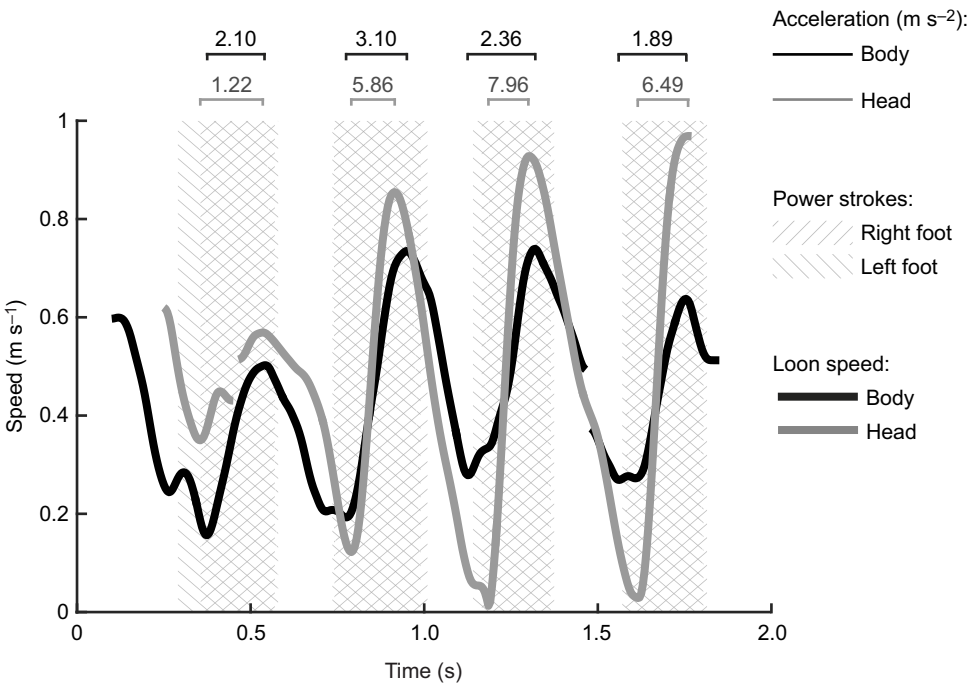

Fig. 4. Body and head speed of a head-bobbing loon. Thick traces show the body (black) and head (gray) speed of a common loon swimming underwater throughout time (*x*-axis). Gaps in the traces represent regions where the view of the tracked feature was obstructed. Cross-hatched panels depict the timing of the right and left power strokes, as determined by observing foot motion. Average acceleration was calculated as the change in speed over the change in time from the lowest speed to the highest speed within a stride. Head bobbing allows loons to stabilize the head, and likely their gaze, during the late recovery stroke. During the early power stroke, as the body accelerates, loons extend the head, reaching accelerations over three times faster than those of the body.

Journal of Experimental Biology (2018) 221, jeb168831. doi:10.1242/jeb.168831

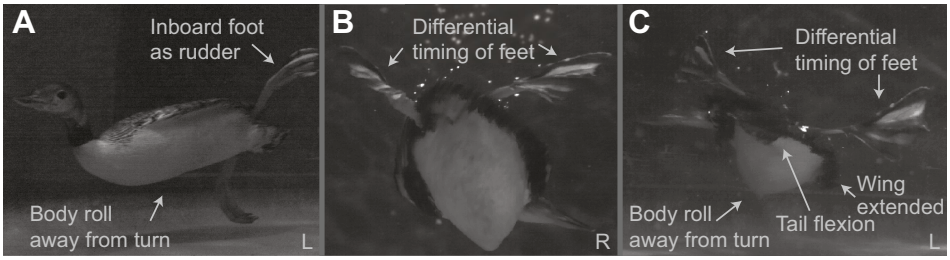

Fig. 5. Observed turning strategies of loons. Still shot frames from three trials (A–C) depict strategies that loons use to turn. 'L' or 'R' in the bottom right corner of each pane denotes the turn direction (left, right). (A) A loon makes a left turn using its inner, left foot as a rudder and rolling its body away from the turn. (B) Turning to the right, a loon varies the timing of its feet. The outboard, left foot began its power stroke earlier and has reached a point behind the loon while the inboard, right foot has only traveled halfway through its power stroke. Though difficult to view from this camera angle, the loon body rolls away from the turn. (C) A loon makes a sharp turn to the left by varying the timing of its feet, extending its outboard wing and depressing its tail. The body of the loon rolls away from the turn.

Stride duration also decreased significantly with increasing speed in all models except for when only considering straight versus outboard foot strides (P=0.134). Lastly, the tip of digit III on the outboard foot traveled a slightly, though not significantly, longer distance throughout the power stroke compared with the inboard foot (~24 versus ~20 cm; Table S4), traveling at a higher average speed (1.06 versus 0.74 m s^{-1}; Table S3). To summarize: (1) the stride of the inboard foot lasted longer than for straight swimming strides, (2) faster swimming loons used shorter stride times and particularly shorter power strokes, and (3) turning loons paddled the outboard foot at a faster average velocity.

Across six turning strides with the hindlimb digitally tracked, loons varied foot motion considerably (Fig. S4). Variation among inboard and outboard strides does not permit a precise description of turning kinematics, but our data reveal some consistent kinematic patterns. During straight swimming, the foot arcs caudally, dorsally and somewhat medially relative to the body through the power stroke (Fig. 7, center). In contrast, for most turning power strokes, the inboard and outboard feet reduce the dorsal component to keep the foot ventral or in line with the ankle (Fig. 7B; Fig. S4). Further, the inboard foot remains caudal to the ankle compared with straight or outboard strides where the foot sometimes reaches a lateral or even cranial position relative to the ankle (Fig. 7A). Two turning strides, one inboard foot (Fig. 7, right) and one outboard foot (Fig. S4, Trial 15), included a larger mediolateral excursion than used during straight swimming. Even though several of the turning strides resembled straight swimming motions, variability among turning strides demonstrates the ability of loons to modulate paddling kinematics and reveals a few potential turning kinematic patterns.

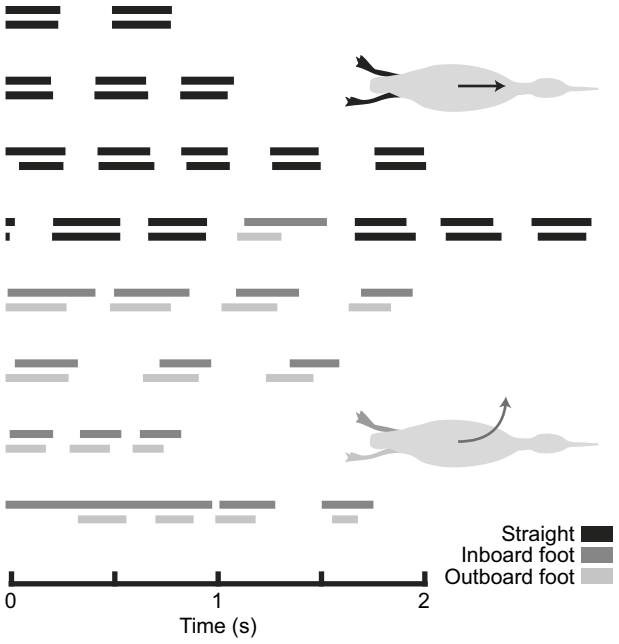

Fig. 6. Power stroke timing of feet during straight swimming and turns. The timing of power strokes was tracked in several trials. Lines represent power strokes with gaps indicating recovery strokes of each foot throughout time (x-axis). Loons generally swim with both feet paddling synchronously, as seen in the straight swimming trials (black). However, during turns, the outboard foot (light gray) consistently begins its power stroke slightly before the inboard foot (dark gray). The trials displayed here show data from both left and right turns, normalized for inboard and outboard feet. In some cases (shown in the bottom trial), the inboard foot was held laterally in a mid-power stroke position, serving as a rudder, while the outboard foot was paddled several times.

DISCUSSION

The large territories of loons and their conservation status pose significant challenges for quantifying their underwater swimming kinematics. Working within a rehabilitation center, we collected detailed 3D data from 19 trials across four healthy individuals, representing both straight swimming and turns. By collecting data over three winter seasons, we were able to demonstrate consistent qualitative, as well as quantitative, findings of these exceptional underwater foot-propelled swimming birds. While observing loons in captivity may underestimate their top swimming speeds, it is unlikely that loons adjust their swimming motions and strategies for turning under confined circumstances. Therefore, we believe that our results report the first detailed analysis of natural loon swimming.

Straight swimming

During straight swimming, we recorded loons reaching speeds up to 0.86 m s^{-1}. Studies analyzing other top foot-propelled swimming birds have recorded faster speeds for straight swimming: 1.2 m s^{-1} in grebes (Johansson and Norberg, 2001) and 1.5–1.7 m s^{-1} in cormorants (Johansson and Norberg, 2003; Ribak et al., 2004; Watanabe et al., 2011). However, these birds were tracked swimming in the wild or through long straight corridors, unlike the comparatively small pool used in this study. We expect that the pool restricted the loons to slower speeds, and that loons likely reach faster speeds in the wild. Further, the loons accelerated up to 1.5 m s^{-1} within straight swimming strides (Table S1), which may contribute to divergence from the relatively steady swimming observed in previous grebe and cormorant studies.

Under the conditions of our study, loons swam using stride frequencies within the range of other foot-propelled swimming

Journal of Experimental Biology (2018) 221, jeb168831. doi:10.1242/jeb.168831

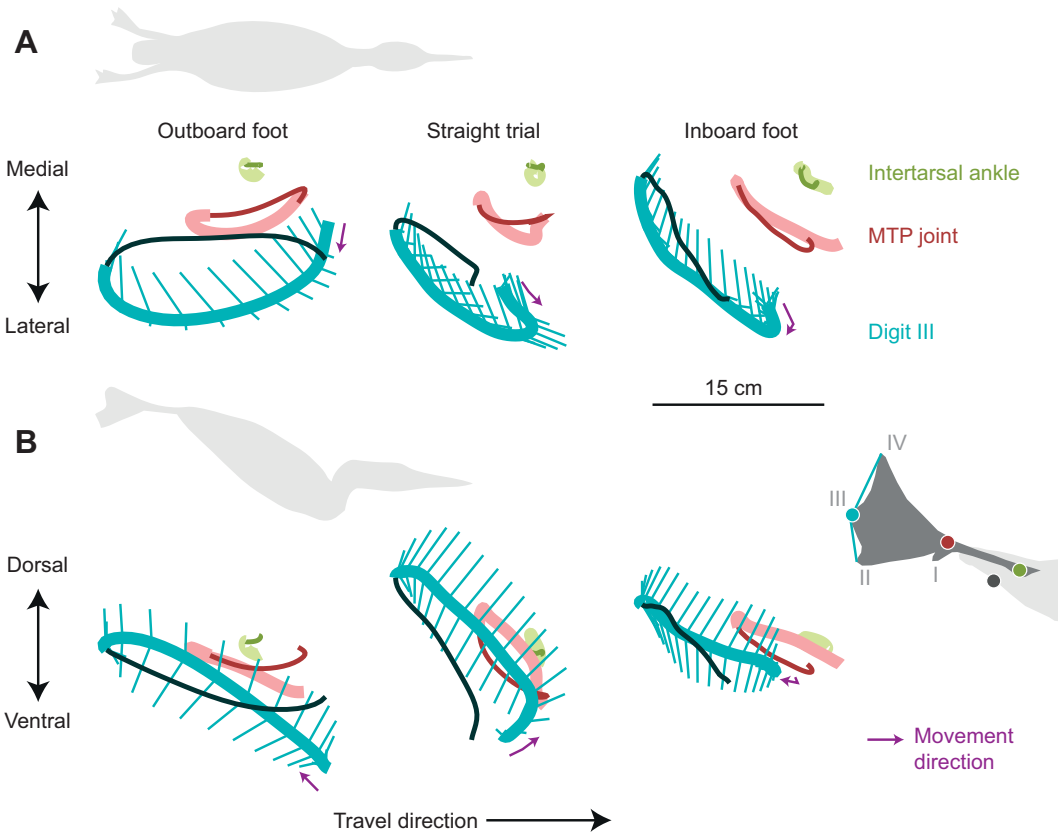

Fig. 7. Right foot motion with respect to the body during straight swimming and turning. The traces show tracked motion relative to the body from a full stride, including the power stroke (thick lines) and recovery stroke (thin lines). Strides from three trials show the foot on the outside of the turn (left, outboard), the foot while swimming in a straight trajectory (center) and the foot on the inside of the turn (right, inboard). The 3D data were rotated to be in reference to the travel direction (*x*-axis), mediolateral plane (A, *y*-axis) and dorsoventral plane (B, *y*-axis), and translated to account for body motion (note, this is a different kinematics representation from that in Fig. 3, in which the foot kinematics are in relation to the water and not the body's motion). (A) View of the right limb from above the loon, showing the intertarsal ankle joint (green), MTP joint (red) and tip of digit III (turquoise). Thin turquoise lines connect the tip of digit III to the tips of digit II and IV every 3rd frame (0.015 s). (B) View of the right limb from the right side of the loon. During the stride for the outboard foot, the loon turned with a radius of curvature (*r*) of 0.09 m and angular velocity (ω) of 247 deg s^{-1}. The turn depicted for the inboard foot stride had *r*=0.49 m and ω=75 deg s^{-1}. The 15 cm scale bar applies to both panels.

birds, but with relatively high values for their body size. When swimming straight, loons used an average stride frequency of 2.04 Hz, similar to values found for grebes (2.50 Hz; Johansson and Norberg, 2001) and cormorants (1.10–3.25 Hz; Ribak et al., 2004; Ribak et al., 2005; Sato et al., 2007; Watanuki et al., 2005). When only comparing values for birds swimming horizontally in captivity, loons swam with faster stride frequencies than those of cormorants despite having a larger body mass (2.9 versus 2.2 kg). Scaling patterns observed within and among aquatic swimmers (Sato et al., 2007, 2010) predict that larger animals should use lower stride frequencies. Therefore, despite swimming with stride frequencies within the range of those of other foot-propelled birds, loons use comparatively fast strides when accounting for body size. This pattern may derive from a relatively small foot area in loons (L. C. Johansson, Lund University, personal communication) or the need to accelerate throughout the stride; however, loons exhibit high stride frequencies even when experiencing low centripetal and tangential accelerations (Table S1, Trial 17).

Despite their relatively high stride frequencies, loons swim with longer power strokes compared with those of other foot-propelled swimming birds. The use of sequential power and recovery strokes in loons is similar to grebes but different from cormorants, which include a gliding phase with their feet held behind the body before each recovery stroke (Ribak et al., 2005). The power stroke of loons approximates 54% of the stride, lasting on average 0.26 s during straight swimming. In comparison, the power strokes of both grebes and cormorants constitute ∼25% of the stride, lasting 0.01 and 0.16 s, respectively (Johansson and Norberg, 2001; Ribak et al., 2004, 2005). As we found that power stroke duration significantly decreases with swim speed, the difference between loons and other swimming birds observed to date could result from the comparatively slow swimming speeds of the loons in the rehabilitation pool used for this study. Finally, loons modulate swim speed primarily by varying their power stroke duration and not stride frequency.

Loons swim by synchronously pushing their feet backward, medially and dorsally during the power stroke, and then drawing the foot forward with collapsed toes during the recovery stroke. However, this paddling is not a simple pivoting motion. The feet begin the power stroke ventral to the body, with the plantar surfaces of the feet facing caudally, but end with the plantar surfaces facing medially towards each other (Fig. 2). The ankle and MTP joints primarily function as a hinge (Stolpe, 1935), suggesting that this rotation of the foot must occur more proximally. Loons have a relatively abducted hip joint with a large antitrochanter that restricts rotation of the femur (Hertel and Campbell, 2007; Wilcox, 1952), likely preventing a contribution of the hip joint to foot rotation.

Instead, foot rotation likely results from rotation at the knee, as has been demonstrated in running birds (Kambic et al., 2014; Kambic et al., 2015). Loons possess an enlarged cnemial crest at the proximal end of the tibiotarsus, which almost completely encloses the anterior and posterior articular surfaces of the distal femur (Wilcox, 1952). While the cnemial crest limits flexion and extension of the knee, it permits long-axis rotation of the tibiotarsus. Grebes demonstrate a similar anatomical pattern, and also swim using long-axis foot rotation while swimming (Johansson and Norberg, 2001). Therefore, loons probably swim by coupling flexion and extension at the ankle joint with rotation at the knee to achieve the net 3D kinematic propulsive and recovery movements of the foot.

The motion of the foot in swimming loons resembles that of grebes, suggesting that loons may also generate lift forces for propulsion. Loons (Figs 2 and 3) and grebes (Johansson and Norberg, 2001) paddle their feet lateral to the body, whereas cormorants paddle their feet ventrally underneath the body (Ribak et al., 2004). Nevertheless, all three underwater swimming species demonstrate almost no motion of the feet opposite to the travel direction relative to the surrounding water (Fig. 3). Because the feet do not substantially push water backward, propulsion cannot depend on drag forces. Instead, loons direct their feet dorsally and medially relative to still water throughout the power stroke. Consequently, this perpendicular motion relative to their travel direction likely produces drag to resist buoyancy and lift for forward propulsion. Although the foot kinematics of loons resembles that of grebes, grebes possess lobate toes that likely act as individual hydrofoils to increase lift production (Johansson and Norberg, 2000). Instead, the webbed feet of loons may enhance lift by functioning like a propeller. As the foot arcs dorsally, the surface of the foot is pitched, leading with digit IV. Lift generated by the angle of attack of the foot would contribute to forward propulsion without moving backward relative to still water. This potential 'propeller' mechanism differs from the proposed 'delta wing' function for cormorant feet (Johansson and Norberg, 2003). By relying on lift instead of drag forces for propulsion, loons can produce propulsive forces at any swim speed, whereas drag-based propulsion is limited to slower speed swimming (Vogel, 2008). Thus, despite variation in whether the feet are moved ventral (cormorants) or lateral (grebes and loons) to the body, three independent lineages of foot-propelled swimming birds indicate the probable use of lift-based propulsion.

Contrary to previous findings (Jimenéz Ortega, 2005), we observed that swimming loons bob their head, likely to enhance their vision. Dozens of bird species across the avian phylogeny exhibit head bobbing while walking, flying or swimming (Jimenéz Ortega, 2005; Ros and Biewener, 2017; Wallman and Letelier, 1993). Head bobbing consists of thrust and hold phases, allowing head (and eye) motion to be dissociated from motion of the body (Necker, 2007). The thrust phase accelerates the head (and eyes) forward relative to the body's motion. The hold phase then allows the head (and eyes) to be held briefly in place, stabilizing the bird's gaze. Head bobbing has been argued to improve vision by increasing depth perception through parallax during the thrust phase, followed by pattern and motion identification during the hold phase (Necker, 2007; Wallman and Letelier, 1993). Prior to our findings, loons were reported not to use head bobbing (Jimenéz Ortega, 2005). Yet, we found clear evidence of head bobbing when loons swim underwater, accelerating their head (and eyes) more than three times faster than their body (Fig. 4; Movie 2). The use of head bobbing while voluntarily diving but not during escape dives suggests its possible use for localizing and pursuing prey. Two other foot-propelled diving birds, grebes (Gunji et al., 2013) and mergansers (Lindroth and Bergstöm, 1959), have also been observed to head bob. Our observation of head bobbing in loons suggests that this behavior may be broadly representative of foot-propelled diving birds, including groups previously considered not to head bob, such as cormorants. Because head bobbing likely enhances vision for hunting prey, it may represent an important function of the comparatively long necks of foot-propelled diving birds.

Turning strategies

Previous studies of foot-propelled swimming birds have focused on swimming through a tunnel or navigating a single vertical obstacle (Johansson and Norberg, 2001; Ribak et al., 2004, 2008). Our study is the first to analyze turning maneuverability of a freely diving foot-propelled bird. Although our findings may not represent the extreme abilities of loons to turn when swimming in the wild because of the confined nature of the swimming pool, we were able to observe maneuvers that likely approach high-level loon turning performance.

Compared with other studied underwater swimmers, the loons in this study executed tight turns but at slow speeds. The minimum radius of curvature observed [0.06 m or 0.07 body lengths (L); Fig. S2], was significantly smaller than that of other diving animals, including sea lions (0.16 m or 0.09 L), penguins (0.14 m or 0.24 L) and cetaceans (0.19 m or 0.15 L) (Fish, 2002; Fish et al., 2003; Hui, 1985). Even so, as a measure of maneuverability, turning curvature does not alone characterize turning performance. The angular rate of change in heading direction serves as a measure of agility, and also influences the ability to capture prey. Loons execute turns at up to 287 deg s^{-1}, more slowly than the maximum rates in sea lions (690 deg s^{-1}) and penguins (576 deg s^{-1}), but comparable to those of dolphins (Fish, 2002), turtles (Rivera et al., 2006) and some teleost fish (average 140–180 deg s^{-1}; Webb and Fairchild, 2001). However, because of the relatively slow swimming speeds that we observed, loons turn with a centripetal acceleration (maximum of 0.2 $\boldsymbol{g}$) much lower than that for sea lions (5.13 $\boldsymbol{g}$) or cetaceans (3.56 $\boldsymbol{g}$). The observation of loons in this study performing sharp but slow turns compared with other underwater hunters may highlight differences in hunting strategy. Sea lions, penguins and cetaceans typically hunt in open water, requiring them to out-chase their prey. In contrast, loons primarily search for prey on the ocean or lake floor, often probing along rocks then quickly snatching any flushed animals (Johnsgard, 1987). This strategy relies on maneuvering in relatively tight spaces, but at slow speeds, until quickly accelerating to capture a fish at close range. Additionally, a potentially important difference between loons and all previously studied turning animals is their long and flexible neck. Limitations to their body's turning ability may not adequately reflect the effective capacity for loons to rotate their head for prey capture. Hunting strategies of loons or other long-necked diving birds have not been quantitatively studied, suggesting an important future direction of this work.

To turn underwater, loons must create a force differential between the sides of their body or redirect the force produced by the feet to produce a swimming torque that rotates the body. There are three main ways that this can be achieved. First, loons could produce stronger propulsive forces on the outboard side relative to the inboard side of the turn. Second, loons could vary the relative timing of force production by each foot. Third, loons could control a turn by redirecting the propulsive forces by altering individual motion of the feet. The following section examines evidence for these turning strategies.

To alter the force produced on each side of the body, loons increase the speed of the outboard relative to the inboard foot. The force each foot produces during the power stroke depends on foot area (abduction of the digits) and speed squared (influenced by both duration of the power stroke and distance traveled by the foot). Because of individual variation and the limited number of turning trials with the foot tracked, no significant evidence was found for more abducted digits on the outboard versus inboard foot. However, loons appear to alter the speed of the outboard foot during the power stroke, modifying both duration and distance relative to still water. Accounting for variation due to swim speed, the power stroke of the outboard foot is significantly shorter than that for the inboard foot during turns (Table S2). The tip of digit III of the outboard foot travels a slightly (but not significantly) longer distance throughout the power stroke, but moves at a significantly faster speed. In more extreme cases of turning, loons dramatically alter inboard versus outboard forces by only paddling the outboard foot or by inducing a backwards drag-based force using the inboard foot as a rudder. These strategies result in a net force acting to rotationally accelerate the loon's body into the turn.

Loons were also observed to paddle the outboard foot before the inboard foot to help initiate and maintain turning. Paddling the outboard foot first amplifies the temporal difference in force between the outboard and inboard sides during the early part of the turn. Any force produced by the outboard foot is transmitted to the body at a point lateral to the bird's center of mass. Without a counteracting force from the inboard foot, the thrust from the outboard foot produces a yaw torque (a rotation around the dorsoventral axis of the bird) into the turn. As the body rotates, the center of mass moves towards the inboard foot, reducing and potentially inverting the yaw moment arm of the inboard foot. The force from the delayed inboard power stroke would then act behind or even outside of the center of mass to sustain the turn.

Our observation that the loon's body rolls outward from the turn is a likely consequence of the temporal offset and differential forces produced by the outboard relative to the inboard foot. Loons experience upward buoyant forces at shallow depths, as evidenced by their tendency to ascend passively. In order to resist buoyancy, each foot must produce a downward force component. Because loons swim with a slight head-down tilt of the body, their center of mass lies vertically below their feet. When the outboard foot paddles earlier and with a greater force than the inboard foot, the downward vertical component of its force acts on the body above and lateral to the center of mass, producing an upward pitch moment and an outward roll moment. As a result, the ventral belly of the loon rotates in toward the turn. Any downward force from the inboard foot will oppose this roll and stabilize the body. In some cases, loons were observed to slightly extend the outboard wing, which would also help to stabilize the body about its roll axis. Many underwater swimmers, including most cetaceans and sea lions, roll into turns to exploit back flexion to increase maneuverability (Fish, 2002; Fish et al., 2003). However, beluga whales and penguins roll out of turns like loons (Fish, 2002; Hui, 1985). Previously, it has been suggested that the body of foot-propelled birds generates a downward-directed lift, which aids turning when the body rolls outward (Johansson, 2002). This benefit of rolling outwards during turns likely applies to loons, and may extend to other swimmers that produce turning forces behind the center of mass.

Turning loons also adjust the 3D motion of their feet to reduce forces that would oppose the turn. While turning, both feet demonstrate a decreased ventral to dorsal component of motion compared with straight swimming (Fig. 7; Fig. S4). With the body rolled away from the turn, any ventrally directed force will point into the turn. Because the forces produced by the feet act on the body behind the center of mass, these ventral forces would induce adverse yaw moments that resist the turn. Reducing dorsoventral motion of the feet during turns therefore serves to limit forces that resist turning.

Conclusions

Loons rely on swimming for hunting, mating and predator evasion. As one of several independent lineages of adept foot-propelled swimming birds, loons provide critical insight into the physical demands, control strategies and evolutionary drivers of swimming. We found that loon swimming resembles that of grebes and likely depends on lift generation for propulsion. Loons modulate the duration of the power stroke when varying swim speed and use head bobbing to enhance underwater vision. Our findings suggest that loons produce propulsive swimming forces convergently to grebe strategies, but diverge from those of cormorants, which retain the ability to walk on land. In the first study to analyze turning in freely swimming foot-propelled birds, we found that loons roll outward from turns and use a combination of paddling mechanisms while turning. Loons increase the speed of the outboard foot, shift the timing of the outboard power stroke to before that of the inboard foot, and vary the individual motions of the inboard versus outboard feet to turn while swimming underwater. These results may provide inspiration for the design and control of swimming robots, with further application to paddling sports.

Acknowledgements

We are grateful to the Tufts Wildlife Clinic, especially Dr Mark Pokras, DVM, and Dr Florina Tseng, DVM, for facilitating this study. We thank Dr Ty Hedrick for helpful conversations, Dr Brendan Jackson for investigated distortion of our camera lenses, and Dr George Lauder for providing tanks to test the underwater camera cases. We are especially grateful to Dr John Hutchinson, Dr Stephanie Pierce and Dr George Lauder for helpful feedback on the manuscript. Two reviewers provided thorough and instrumental comments for improving the manuscript. Lastly, we would like to thank the personnel at the Concord Field Station.

Competing interests

The authors declare no competing or financial interests.

Author contributions

Conceptualization: G.T.C.; Methodology: G.T.C.; Software: G.T.C.; Formal analysis: G.T.C.; Data curation: G.T.C.; Writing - original draft: G.T.C.; Writing - review & editing: A.A.B.; Supervision: A.A.B.

Funding

The research presented in this paper was funded through internal graduate research allowances to G.T.C. through the department of Organismal and Evolutionary Biology at Harvard University.

Data availability

Stride timing and 3D tracked mat files are provided in the Harvard Dataverse: https://doi.org/10.7910/DVN/MYGSYO.

Supplementary information

Supplementary information available online at
http://jeb.biologists.org/lookup/doi/10.1242/jeb.168831.supplemental

References

Abourachid, A. (2001). Kinematic parameters of terrestrial locomotion in cursorial (ratites), swimming (ducks), and striding birds (quail and guinea fowl). *Comp. Biochem. Physiol. A Mol. Integr. Physiol.* **131**, 113-119.

Barr, J. F. (1996). Aspects of Common Loon (Gavia immer) feeding biology on its breeding ground. *Hydrobiologia* **321**, 119-144.

Baudinette, R. V. and Gill, P. (1985). The energetics of "flying" and "paddling" in water: locomotion in penguins and ducks. *J. Comp. Physiol. B* **155**, 373-380.

Blake, R. W. (1981). Mechanics of drag-based mechanisms of propulsion in aquatic vertebrates. *Symp. Zool. Soc. London* **48**, 29-52.

Chinsamy, A., Martin, L. D. and Dobson, P. (1998). Bone microstructure of the diving Hesperornis and the voltant Ichthyornis from the Niobrara Chalk of western Kansas. *Cretac. Res.* **19**, 225-235.
Clifton, G. T., Carr, J. A. and Biewener, A. A. (2018). Comparative hindlimb myology of foot-propelled swimming birds. *J. Anat.* **232**, 105-123.
Fish, F. (1996). Transitions from drag-based to lift-based propulsion in mammalian swimming. *Am. Zool.* **36**, 628-641.
Fish, F. E. (2002). Balancing requirements for stability and maneuverability in cetaceans. *Integr. Comp. Biol.* **42**, 85-93.
Fish, F. E. and Nicastro, A. J. (2003). Aquatic turning performance by the whirligig beetle: constraints on maneuverability by a rigid biological system. *J. Exp. Biol.* **206**, 1649-1656.
Fish, F. E., Hurley, J. and Costa, D. P. (2003). Maneuverability by the sea lion Zalophus californianus: turning performance of an unstable body design. *J. Exp. Biol.* **206**, 667-674.
Grémillet, D., Chauvin, C., Wilson, R. P., Le Maho, Y. and Wanless, S. (2005). Unusual feather structure allows partial plumage wettability in diving great cormorants Phalacrocorax carbo. *J. Avian Biol.* **36**, 57-63.
Gunji, M., Fujita, M. and Higuchi, H. (2013). Function of head-bobbing behavior in diving little grebes. *J. Comp. Physiol. A. Neuroethol. Sens. Neural. Behav. Physiol.* **199**, 703-709.
Hertel, F. and Campbell, K. E., Jr. (2007). The antitrochanter of birds: form and function in balance. *Auk* **124**, 789-805.
Hui, C. A. (1985). Maneuverability of the Humboldt penguin (Spheniscus humboldti) during swimming. *Can. J. Zool.* **63**, 2165-2167.
Jimenéz Ortega, L. (2005). Avian visual perception: interocular and intraocular transfer and head-bobbing behaviour in birds. *PhD thesis*, International Graduate School of Neuroscience (IGSN), Ruhr-University Bochum, Germany.
Johansson, L. (2002). Swimming in birds. Propulsive mechanisms and functional morphology. *DPhil thesis*, Göteborg University, Sweden.
Johansson, L. C. and Norberg, U. M. (2000). Asymmetric toes aid underwater swimming. *Nature* **407**, 582-583.
Johansson, L. and Norberg, U. M. (2001). Lift-based paddling in diving grebe. *J. Exp. Biol.* **204**, 1687-1696.
Johansson, L. C. and Norberg, R. (2003). Delta-wing function of webbed feet gives hydrodynamic lift for swimming propulsion in birds. *Nature* **424**, 65-68.
Johnsgard, P. A. (1987). *Diving Birds of North America*. Lincoln, Nebraska: University of Nebraska Press.
Kambic, R. E., Roberts, T. J. and Gatesy, S. M. (2014). Long-axis rotation: a missing degree of freedom in avian bipedal locomotion. *J. Exp. Biol.* **217**, 2770-2782.
Kambic, R. E., Roberts, T. J. and Gatesy, S. M. (2015). Guineafowl with a twist: asymmetric limb control in steady bipedal locomotion. *J. Exp. Biol.* **218**, 3836-3844.
Lindroth, A. and Bergstöm, E. (1959). Notes on the feeding technique of the Goosander in streams. *Inst. Freshw. Res.* **40**, 165-175.
Miller, R. E. and Fowler, M. E. (2014). *Fowler's Zoo and Wild Animal Medicine*. Vol. 8. St. Louis, Missouri: Elsevier Health Sciences.
Necker, R. (2007). Head-bobbing of walking birds. *J. Comp. Physiol. A. Neuroethol. Sens. Neural. Behav. Physiol.* **193**, 1177-1183.
Nocera, J. J. and Burgess, N. M. (2002). Diving schedules of Common Loons in varying environments. *Can. J. Zool.* **80**, 1643-1648.
Ribak, G., Weihs, D. and Arad, Z. (2004). How do cormorants counter buoyancy during submerged swimming? *J. Exp. Biol.* **207**, 2101-2114.
Ribak, G., Weihs, D. and Arad, Z. (2005). Submerged swimming of the great cormorant Phalacrocorax carbo sinensis is a variant of the burst-and-glide gait. *J. Exp. Biol.* **208**, 3835-3849.
Ribak, G., Weihs, D. and Arad, Z. (2008). Consequences of buoyancy to the maneuvering capabilities of a foot-propelled aquatic predator, the great cormorant (Phalcrocorax carbo sinensis). *J. Exp. Biol.* **211**, 3009-3019.
Rivera, G., Rivera, A. R. V., Dougherty, E. E. and Blob, R. W. (2006). Aquatic turning performance of painted turtles (Chrysemys picta) and functional consequences of a rigid body design. *J. Exp. Biol.* **209**, 4203-4213.
Ros, I. G. and Biewener, A. A. (2017). Pigeons (C. livia) follow their head during turning flight: head stabilization underlies the visual control of flight. *Front. Neurosci.* **11**, 655.
Sato, K., Watanuki, Y., Takahashi, A., Miller, P. J. O., Tanaka, H., Kawabe, R., Ponganis, P. J., Handrich, Y., Akamatsu, T., Watanabe, Y. et al. (2007). Stroke frequency, but not swimming speed, is related to body size in free-ranging seabirds, pinnipeds and cetaceans. *Proc. R. Soc. B Biol. Sci.* **274**, 471-477.
Sato, K., Shiomi, K., Watanabe, Y., Watanuki, Y., Takahashi, A. and Ponganis, P. J. (2010). Scaling of swim speed and stroke frequency in geometrically similar penguins: they swim optimally to minimize cost of transport. *Proc. Biol. Sci.* **277**, 707-714.
Schorger, A. (1947). The deep diving of the loon and old-squaw and its mechanism. *Wilson Bull.* **59**, 151-159.
Sidor, I. F., Pokras, M. A., Major, A. R., Poppenga, R. H., Taylor, K. M. and Miconi, R. M. (2003). Mortality of common loons in New England, 1987 to 2000. *J. Wildl. Dis.* **39**, 306-315.
Stolpe, M. (1935). Colymbus, Hesperornis, Podiceps: ein Vergleich ihrer hinteren Extremität. *J. Ornithol.* **83**, 115-128.
Taubin, G. (1991). Estimation of planar curves, surfaces, and nonplanar space curves defined by implicit equations with applications to edge and range image segmentation. *IEEE Trans. Pattern Anal. Mach. Intell.* **13**, 1115-1138.
Theriault, D. H., Fuller, N. W., Jackson, B. E., Bluhm, E., Evangelista, D., Wu, Z., Betke, M. and Hedrick, T. L. (2014). A protocol and calibration method for accurate multi-camera field videography. *J. Exp. Biol.* **217**, 1843-1848.
Vogel, S. (2008). Modes and scaling in aquatic locomotion. *Integr. Comp. Biol.* **48**, 702-712.
Wallman, J. and Letelier, J.-C. (1993). Eye movements, head movements, and gaze stabilization in birds. In *Vision, Brain, and Behavior in Birds* (ed. H. P. Zeigler and H.-J. Bischof), pp. 245-263. Cambridge, MA: The MIT Press.
Watanabe, Y. Y., Sato, K., Watanuki, Y., Takahashi, A., Mitani, Y., Amano, M., Aoki, K., Narazaki, T., Iwata, T., Minamikawa, S. et al. (2011). Scaling of swim speed in breath-hold divers. *J. Anim. Ecol.* **80**, 57-68.
Watanuki, Y., Takahashi, A., Daunt, F., Wanless, S., Harris, M., Sato, K. and Naito, Y. (2005). Regulation of stroke and glide in a foot-propelled avian diver. *J. Exp. Biol.* **208**, 2207-2216.
Webb, P. W. (1988). Simple physical principles and vertebrate aquatic locomotion. *Am. Zool.* **28**, 709-725.
Webb, P. W. and Fairchild, A. G. (2001). Performance and maneuverability of three species of teleostean fishes. *Can. J. Zool.* **79**, 1866-1877.
White, C. R., Martin, G. R. and Butler, P. J. (2008). Pedestrian locomotion energetics and gait characteristics of a diving bird, the great cormorant, *Phalacrocorax carbo*. *J. Comp. Physiol. B.* **178**, 745-754.
Wilcox, H. H. (1952). The pelvic musculature of the loon, *Gavia immer*. *Am. Midl. Nat.* **48**, 513-573.
Zinoviev, A. V. (2011). Notes on the hindlimb myology and syndesmology of the Mesozoic toothed bird *Hesperornis regalis* (Aves: Hesperornithiformes). *J. Syst. Palaeontol.* **9**, 65-84.

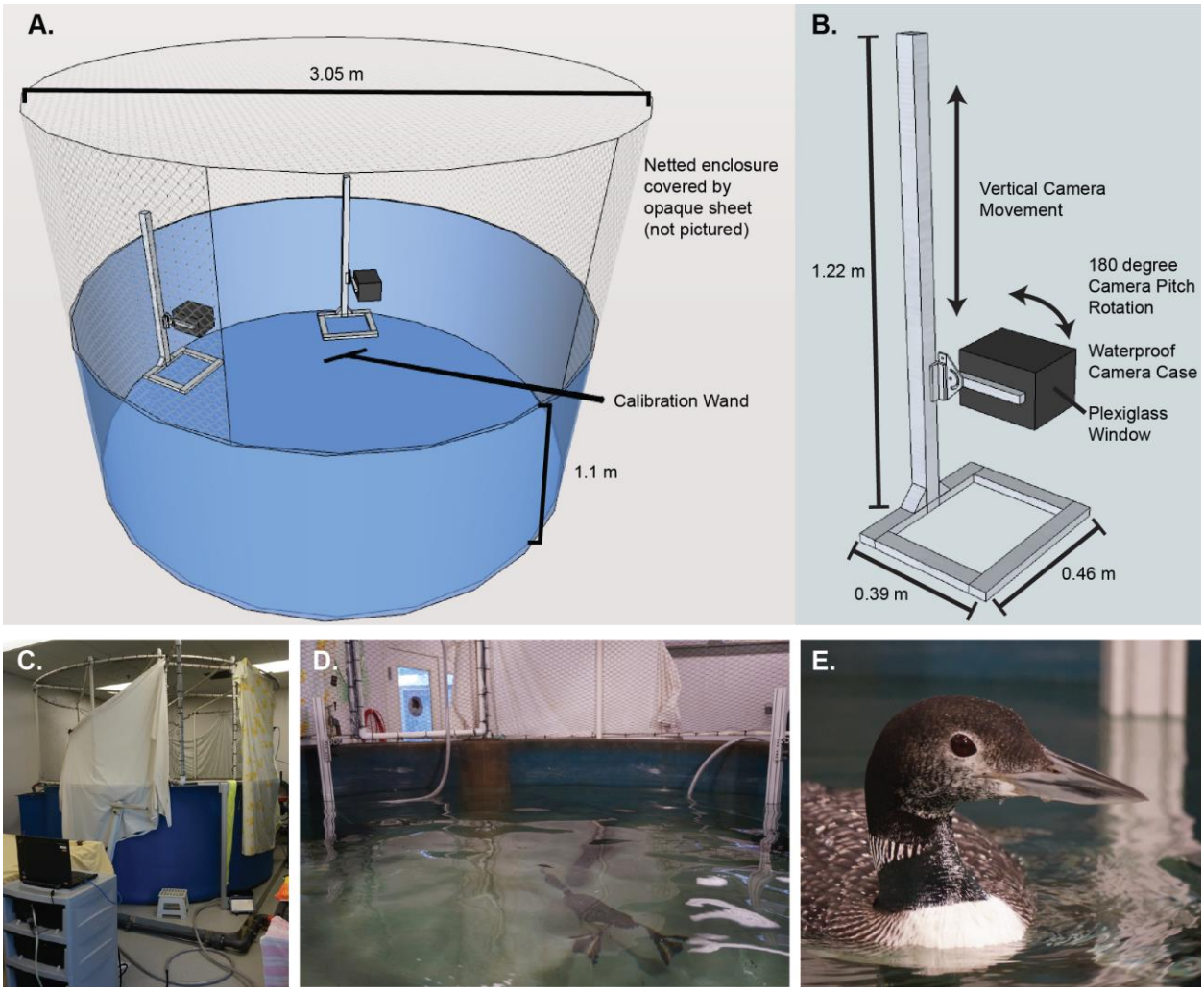

Figure S1. **Filming set-up at the Tufts Wildlife Clinic.** (A) Two cameras were placed in a 3.3 m diameter pool, where rehabilitating loons were housed. A calibration wand was used to calibrate the area for 3D reconstruction. (B) Custom camera cases and stands were built for IDT NR5S1 cameras. Scuba dive boxes were outfitted with a Plexiglass window, removable camera mount, and plumbing tube (to waterproof and protect the camera's cable to its power box). The stand was built using 80/20 aluminum framing. (C) While recording, a sheet was placed over the netting to reduce loons stress levels. (D) Loons voluntarily swam underwater in the field of view of both cameras. (E) All four common loons were healthy and released to the wild within 24 hours of recording.

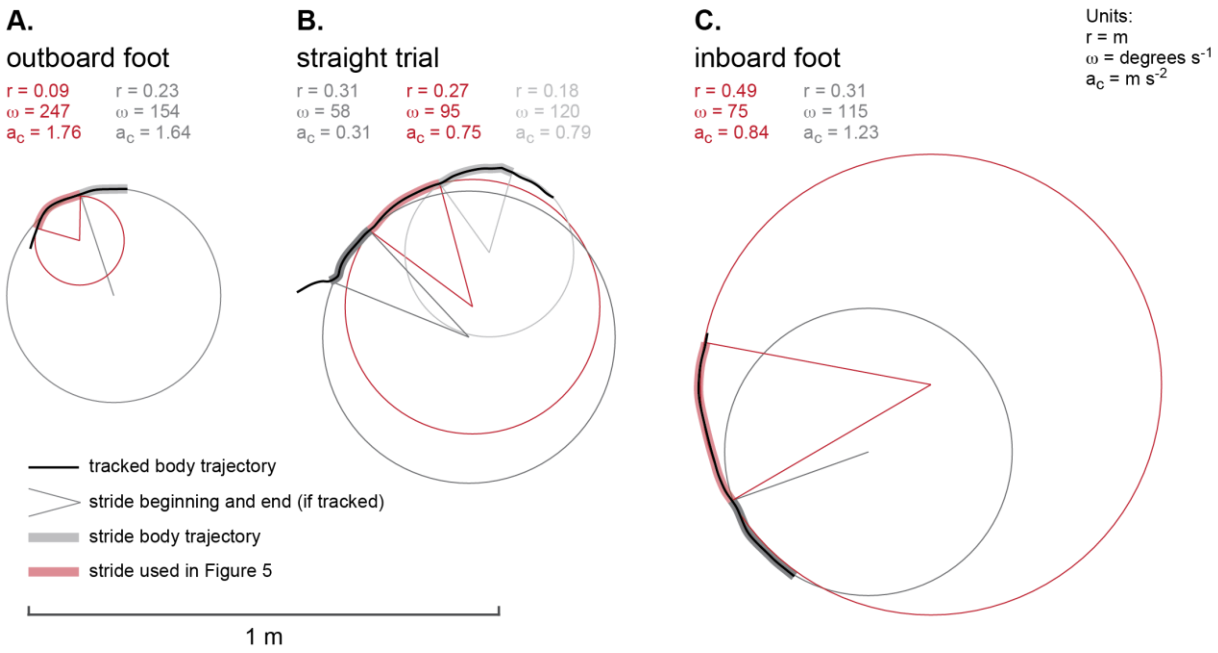

Figure S2. **Analysis of turns using body trajectory data from strides shown in Figure 5.** Maneuverability and agility were determined by analyzing the trajectory of the loon's body during individual strides. For each stride where over 70% of the stride was tracked, a circle was fit to the horizontal traces of the body. The radius of the curvature (r), angular velocity (ω), and centripetal acceleration (a_c) were calculated for each stride. The panels in this figure represent the strides displayed in Fig. 5 (red) for (A) a turn with the outboard foot tracked, (B) straight swimming, and (C) a turn with the inboard foot tracked. All panels are scaled to the 1 m scale bar.

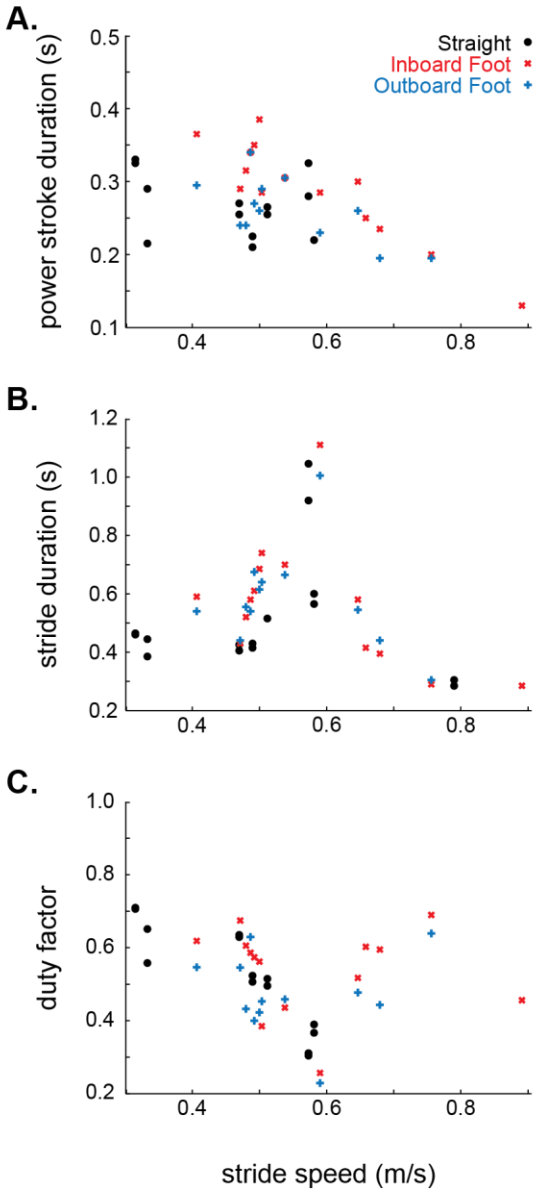

Figure S3. Kinematic parameters for straight swimming and turning strides versus swimming speed. The timing of paddling was calculated for over 100 strides from 19 trials. Body speed was tracked during 23 full strides, corresponding to 46 potential foot paddles. Based on the visibility in the video recordings for each foot paddle, the following kinematic parameters were calculated: (A) power stroke duration, (B) stride duration, and (C) duty factor, or the fraction of the full stride used for the power stroke. Linear mixed effects models were fit to the data incorporating errors from individual variation as well as the impact of speed and foot type category. Statistical analyses were repeated comparing straight (black circles) versus inboard foot (red "x") versus outboard foot (blue "+") data and while binning together inboard and outboard strides as all turning data.

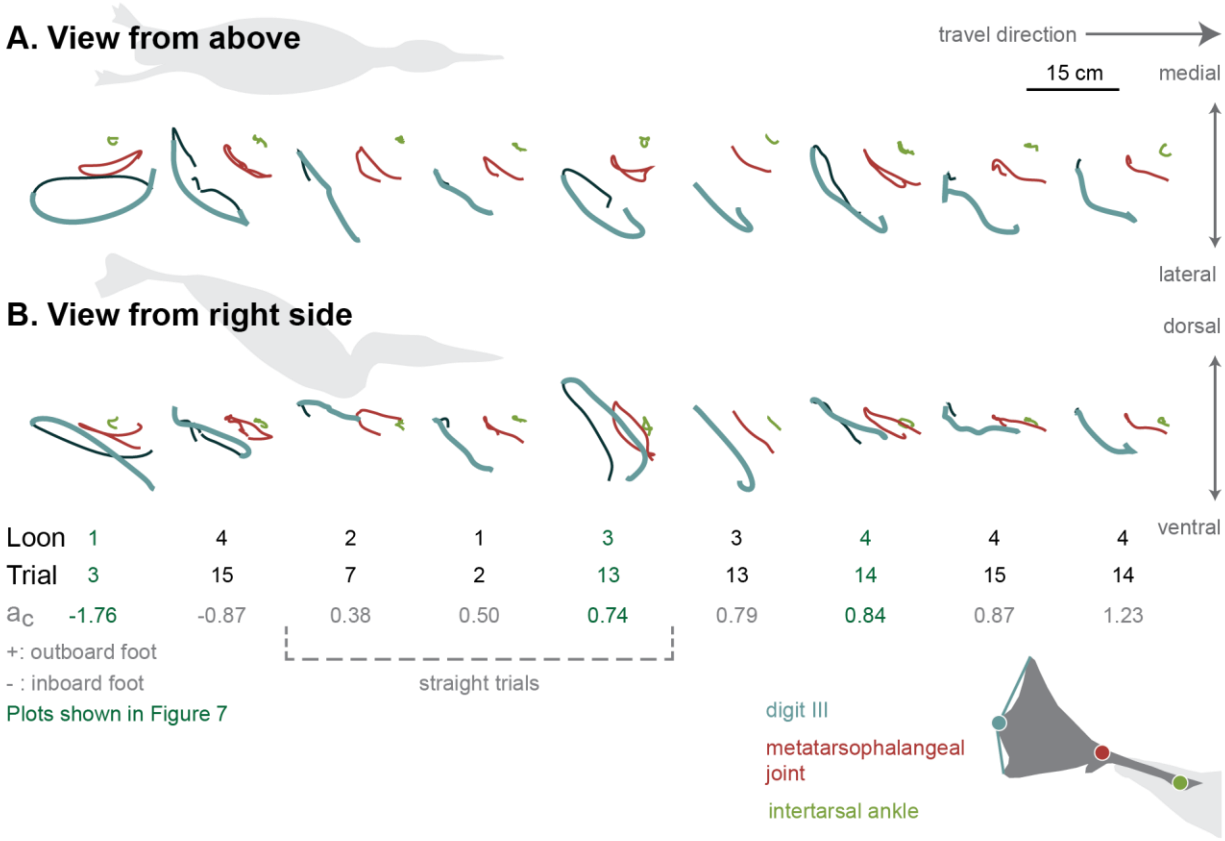

Figure S4. Foot motion variability during straight swimming and turning. The traces show tracked motion *relative to the body* including the power stroke (thick, light turqoise) and recovery stroke (thin dark blue). Strides are arranged by turn centripetal force with outboard feet represented by negative acceleration values and inboard feet represented by positive values. To improve comparisons, all tracked left feet have been reflected across the sagittal plane to appear as right feet. The 3D data are rotated to be in reference to the travel direction (x-axis), mediolateral plane (A, y-axis), and dorsoventral plane (B, y-axis) and translated to account for body motion. (A) View of the 'right' limb from above the loon showing the intertarsal ankle joint (green), metatarsophalangeal joint (MTP, red), and tip of digit III (blue). (B) View of the 'right' limb from the right side of the loon. All panels scaled to 15 cm scale bar. Trial information listed in dark green represents trials represented in Figure 7.

Table S1. Stride turning parameters in the horizontal plane. In 19 trials with body tracking, a circle was fit to the horizontal trajectory during each stride with at least 30% of the stride tracked. The circle fit provided an average radius of curvature, *r*, which was used to calculate average angular velocity, ω, and average centripetal acceleration a_c. The tangential acceleration, a_t, is defined as $a_t = r * \alpha$, where α is the average angular acceleration. α was calculated by finding the average $\Delta(\omega_{instantaneous})/\Delta t = \Delta(u_{instantaneous})/(r*\Delta t)$. The tracked foot column identifies 9 strides with reliable 3D foot tracking of an inboard (IB), outboard (OB) or straight swimming (SS) stride. The average stride duration of both limbs is shown for each stride when available.

Loon	Trial	*r* (m)	*u* (m s^{-1})	ω (deg s^{-1})	a_c (m s^{-2})	a_t (m s^{-2})	tracked feet	st. dur (s)
1	1	0.448	0.54	68.39	0.639	0.074		0.68
		0.458	0.52	65.07	0.590	0.123		0.62
	2	0.207	0.48	132.18	1.100	-0.023		0.54
		0.475	0.49	58.75	0.499	0.156	SS	0.69
	3	0.228	0.61	153.70	1.638	-1.782		0.33
		0.095	0.41	246.93	1.762	-0.215	OB	0.30
	4	0.274	0.36	74.85	0.467	-0.563		0.51
		0.404	0.40	56.27	0.389	0.019		0.57
		0.549	0.45	46.94	0.368	1.153		0.61
2	5	0.269	0.64	136.68	1.530	-0.585		0.69
		2.908	0.64	12.53	0.139	-0.010		0.89
	6	0.395	0.54	77.61	0.726	-0.407		0.75
		0.240	0.55	130.49	1.245	0.680		0.39
	7	0.860	0.57	37.91	0.376	0.033	SS	0.98
	8	0.449	0.70	89.61	1.097	-1.057		0.28
		0.122	0.44	204.57	1.559	-0.618		0.56
	9	0.463	0.55	67.46	0.642	-0.109		1.08
3	10	0.428	0.26	35.00	0.160	-0.999		
		0.339	0.30	50.26	0.261	0.412		0.46
	11	1.518	0.59	22.26	0.229	1.501		0.43
	12	1.860	0.50	15.26	0.132	-0.657		0.52
	13	0.311	0.31	57.68	0.315	-0.184		0.42
		0.271	0.45	95.03	0.745	0.218	SS	0.42
		0.179	0.38	120.08	0.788	-0.105	IB	0.43
		0.300	0.36	69.37	0.440	0.713		0.50
4	14	0.491	0.64	75.05	0.842	0.136	IB	0.56
		0.306	0.61	115.11	1.234	0.173	IB	0.60
	15	0.252	0.49	110.23	0.934	0.123		0.64
		0.278	0.49	101.63	0.874	0.020	IB & OB	0.65
	16	0.178	0.59	188.30	1.928	-0.234		0.42
		0.230	0.66	164.67	1.904	0.367		0.42
	17	1.145	0.66	33.02	0.380	-0.420		0.30
		0.455	0.60	75.72	0.794	1.789		0.34
	18	6.588	0.55	4.83	0.047	-0.588		0.58
		0.589	0.45	44.08	0.349	-0.083		0.44
	19	0.061	0.31	287.49	1.545	1.053		0.53

Table S2. Means and standard errors of kinematic parameters of loon swimming. In 19 recorded trials of loons swimming freely underwater the timing of foot paddling and body speed were tracked. The table shows the average and error values for several kinematic parameters for all strides and decomposed into three swim-type categories: strides where the loon was swimming straight, turning strides with the inboard foot tracked, and turning strides with the outboard foot tracked. The n columns show how many strides were analyzed for each kinematic parameter and swim-type category.

	All trials			Straight Strides			Inboard Foot			Outboard Foot		
	n	Mean	Std. Error	n	Mean	Std. Error	n	Mean	Std. Error	n	Mean	Std. Error
Power stroke time (s)	112	0.265	0.005	32	0.258	0.006	40	0.279	0.011	40	0.2568	0.008
Stride time (s)	80	0.546	0.020	26	0.487	0.032	28	0.578	0.036	26	0.569	0.032
Duty factor	77	0.513	0.015	24	0.542	0.024	27	0.521	0.029	26	0.478	0.023
Stride speed (m s^{-1})	23	0.542	0.031	9	0.484	0.053	5	0.637	0.076	9	0.546	0.035

Table S3. Likelihood ratio tests for linear mixed effects models of loon swimming kinematic parameters. To account for swim-type category, stride body speed, and individual loon variation, linear mixed-error models were applied to kinematic parameters. Swim-type category (straight swimming strides, turning strides tracking the inboard foot, and turning strides tracking the outboard foot) and stride body speed were fixed effects, with loon identity as a random effect. Likelihood ratio tests compared full models to a model with either the swim-type or speed effect removed, calculating a p-value representing the influence of that effect on the kinematic parameter. These values are listed in the table (all non-"n" columns). Bold p-values denote significance using a 0.05 cut-off.

	straight vs. inboard vs. outboard			**straight vs. inboard**			**straight vs. outboard**			**inboard vs. outboard**			**straight vs. turning (in- + outboard)**		
	n	**swim type**	**speed**	**n**	**swim type**	**speed**	**n**	**swim type**	**speed**	**n**	**swim type**	**speed**	**n**	**swim type**	**speed**
Power stroke time (s)	40	1	**3.5e-5**	28	**0.007**	**2.5e-5**	26	1	**0.018**	26	0.156	**6.1e-7**	40	1	**1.4e-5**
Stride time (s)	42	1	**0.004**	30	1	**0.005**	28	1	0.134	26	1	**0.028**	42	1	**0.003**
Duty factor	40	1	1	28	0.148	0.890	26	1	0.330	26	1	1	40	1	1

Table S4. Digit III speed and travel distance during straight and turning strokes. The total distance traveled and average speed of the tip of digit III was calculated for 9 strokes, three during straight swimming and six while turning.

	Loon	Trial	a_c (m s^{-2})	Dig III distance (m)	Digiti III speed (m/s)
Straight	1	2	0.499	0.1460	0.5120
	2	7	0.376	0.1966	0.6049
	3	13	0.745	0.2437	0.9025
mean				*0.1954*	*0.6731*
Inboard foot	3	13	0.788	0.1978	0.9418
	4	14	0.842	0.2181	0.7270
	4	14	1.234	0.1820	0.7582
	4	15	0.874	0.2067	0.5370
mean				*0.2011*	*0.7410*
Outboard foot	1	3	1.762	0.2379	1.2197
	4	15	0.874	0.2337	0.8989
mean				*0.2358*	*1.0593*

Movie S1 – Underwater swimming by a common loon. The loon was filmed in a rehabilitation pool at the Tufts Wildlife Clinic. Footage was recorded at 200fps and is played back at 30fps, appearing 6.7 times slower than real life.

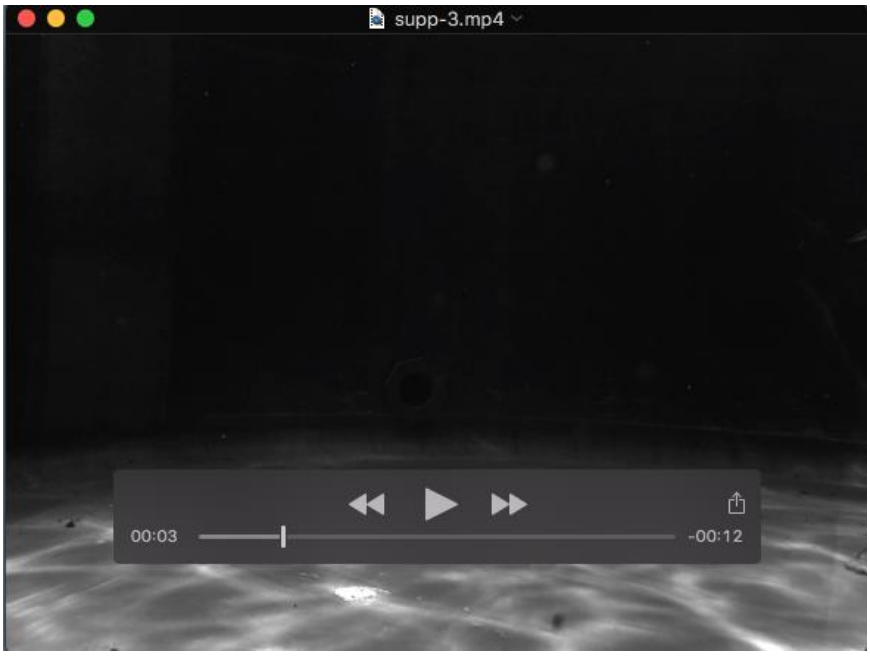

Movie S2 – Head-bobbing by a diving common loon. The loon was filmed in a rehabilitation pool at the Tufts Wildlife Clinic. Footage was recorded at 200fps and is played back at 30fps, appearing 6.7 times slower than real life.

Movie S3 – Tracked maneuvers by diving common loons. The loons were filmed in a rehabilitation pool at the Tufts Wildlife Clinic. Footage was recorded at 200fps and is played back at 30fps, appearing 6.7 times slower than real life. All clips have been digitally tracked for body motion or body and foot motion.